

HIGH RESOLUTION AND DYNAMIC RANGE CHARACTERISATION OF BEAM IMAGING SYSTEMS

J. Wolfenden[†], R. Fiorito, C.P. Welsch, Cockcroft Institute and The University of Liverpool, UK
 P. Karataev, K. Kruchinin, JAI at Royal Holloway University of London, Egham, UK
 M. Bergamaschi, R. Kieffer, T. Lefevre, S. Mazzoni, CERN, Geneva, CH

Abstract

All imaging techniques require the use of optical components to transfer light from a source to a sensor. The impact of the transfer optics on the image resolution is often not well understood. To improve this situation, the point spread function (PSF) of the optical system needs to be measured; this requires a good point source and sufficient dynamic range to fully characterize the PSF distribution. For this purpose we have created an intense optical point source, using a high quality laser and special focusing optics. The PSFs of various optical systems, developed for high resolution electron beam imaging, were measured using this source and compared to Zemax simulations. These systems incorporate a digital micro-mirror array, which was used to produce very high ($>10^5$) dynamic range images. The goal is to systematically understand and mitigate any ill effects due aberrations, diffraction, and misalignments of all the components of the imaging system. Presented here are the results of our measurements and simulations.

INTRODUCTION

The effect an optical system has on an image is often ignored or approximated. This uncertainty can result in a restriction in the precision of the measurement and ultimately to a loss of resolution. In high resolution imaging systems, such as those using OTR to determine the size of micron size electron beams [1], the effect of the PSF of the optics is particularly important. Optical PSFs usually take the form of a distribution with a central maximum, such as a Gaussian, Airy, Lorentzian, etc. The resolution of such systems are commonly determined by the FWHM of these distributions. The OTR PSF of a single electron is distinct, in that it contains a zero valued central minimum. An example [2] is presented in Fig. 1. The detailed shape of the OTR PSF, particularly the central minimum region, allows an effective resolution to be achieved that is much smaller than the FWHM of the PSF. The OTR image of an electron distribution with a width comparable to the FWHM of the PSF displays a central minimum, but with a finite non-zero value. An example of this for a 1 μm electron beam is also presented in Fig. 1 for comparison. The change in the depth of the minimum is due to the convolution of the transverse profile of the electron beam and the single electron OTR PSF. Therefore, if the theoretically calculable OTR PSF for a single electron [2] can be removed from the measured OTR distribution, a previously unattainable level of resolution on beam size measurements can be achieved. However, the optical system

used to image the OTR will have an intrinsic PSF, due to diffraction and aberrations of the individual elements in the system. The optical PSF will broaden the OTR PSF degrading the resolution for the beam size measurements.

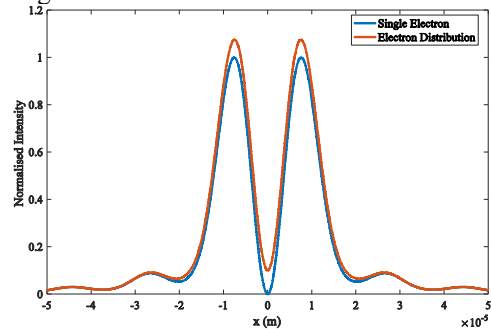


Figure 1: Examples of a single electron OTR PSF and an electron distribution OTR PSF.

If the performance of the optics were assessed separately, then it would be possible to deconvolve the optical PSF from the measured OTR profiles; thus improving the resolution attainable. The beam measurements made with OTR are sensitive to not only the central minimum, but to the entire shape of the PSF [1]. It follows that if the low intensity details of the OTR distribution were imaged with the high intensity central region, the deconvolution procedure would be improved. These details can be revealed by implementing high dynamic range (HDR) imaging, which will also improve the signal to noise ratio in the central minimum. This would further increase the resolution of the beam diagnostic measurements utilising OTR. A digital micro-mirror array (DMD) can be employed to provide HDR imaging, however the effect of the DMD on the PSF must be quantified.

POINT SOURCE CHARACTERISATION

Point Source Creation

To carry out a true PSF measurement it is necessary to have a point source. A practical approximation for this theoretical construct is a uniform distribution of light emanating from a small point of finite volume, e.g. a star. This effect was emulated by using a technique developed for laser-wire diagnostics [3], where a high-quality laser is focused to a small spot. This focal spot is the effective point source. A high-quality laser is required to ensure a high-quality focus point. To this end, the M^2 value [4] of the laser was measured and used as an indicator of its quality. This is an intrinsic property of the laser and is an indicator of its ability to produce a low divergence beam with a Gaussian transverse profile. The measurement was achieved by directly using a CCD to take a statistical

[†] joseph.wolfenden@liverpool.ac.uk

measure known as the $D4\sigma$ waist. This is equivalent to e^{-2} for a Gaussian beam. Figure 2 displays the results of these measurements as a function of longitudinal position.

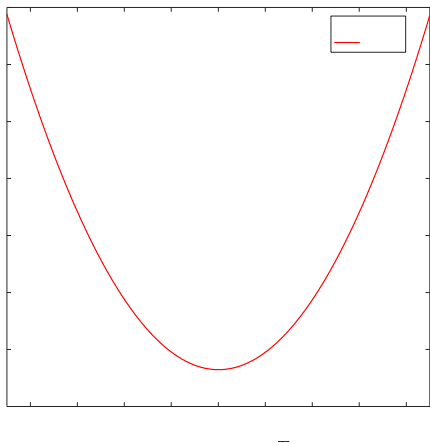


Figure 2: The waist of the laser as a function of longitudinal position.

Equation (1) was used to produce the theoretical fit shown in Fig. 2:

$$\omega^2 = \omega_0^2 + \left(\frac{M^2\lambda}{\pi\omega_0}\right)^2 (z - z_0)^2 \quad (1)$$

where ω is the beam waist, ω_0 is the minimum beam waist and z_0 is the position of the minimum. This provided a value of $M^2 = 1.31 \pm 0.23$. As this was comparable to the optimum value of 1, it was a positive indication of the lasers' ability to achieve a diffraction limited focal spot. Equation (2) is the theoretical calculation of the diffraction limited spot size for a single focussing optic [5]:

$$\omega_0 = \frac{2f\lambda}{D} = \frac{2f\lambda}{\pi d} \quad (2)$$

where f is the focal length of the focussing optic, D is the diameter of the focussing optic and d is the diameter of the input beam. The element selected was a 50.8 mm aspheric lens to reduce spherical aberrations. Equation (2) makes use of the approximation $D = \pi d$, where 99% of the light is captured with a 1% loss of resolution due to diffraction [5]. Equation (2) predicts a diffraction limited spot size of $1.33 \mu\text{m}$ for a 32 mm input beam. A 16X beam expander was placed prior to the focussing lens to provide the 32 mm input from an initial 2 mm beam.

Size Measurement

The size of the point source could not be directly measured, as the spot size was less than the size of any sensor pixel. To probe this small area a knife edge scan was used [6]. This consisted of performing a high resolution scan of a single edged knife across the transverse beam profile, whilst monitoring the intensity of the unimpeded light. A measurement of ω was achieved by fitting an error function to the sigmoid shaped data, and differentiating this to find the e^{-2} waist of the corresponding Gaussian. A picture of the evolution of the beam waist was built up by repeat-

ing this process throughout the depth of focus. An indirect measurement of $\omega_0 = (1.34 \pm 0.01) \mu\text{m}$ was achieved by fitting Equ. (1) to this data. This was comparable to the theoretically predicted diffraction limited spot size, indicating that the optics used to produce this point source are near optimal.

OPTICAL SYSTEM PERFORMANCE

OTR Imaging System

The OTR imaging system employed for analysis was a simple single lens imaging system. The lens was a plano-convex singlet with a focal length of 30.1 mm and a diameter of 12.7 mm. With the position of the point source known from the knife edge scan, the lens was positioned to provide a magnification of 14, which was verified using a resolution target. Figure 3 is a diagram of the optical system. The resolution target also provided a minimum resolvable size of $3.48 \mu\text{m}$, which is an estimate of the resolution of the system.

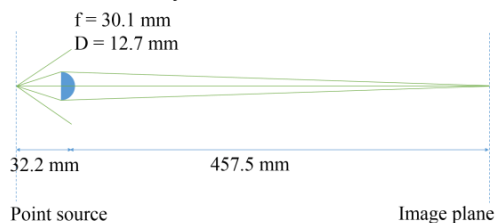


Figure 3: Schematic of the simple lens imaging optics.

The PSF of the OTR imaging system was then determined by directly imaging the point source. The FWHM of this distribution was $(2.99 \pm 0.01) \mu\text{m}$, which is an independent measurement of the resolution of the optical system. The PSF profile, the theoretical fit for an Airy disk, and the PSF from simulations of the optical system in Zemax Optical Studio (ZOS) are presented in Fig. 4. The agreement found between the FWHM of the measured PSF, the estimate from the resolution target and the simulations in ZOS, provides a level of validity to the PSF measurement.

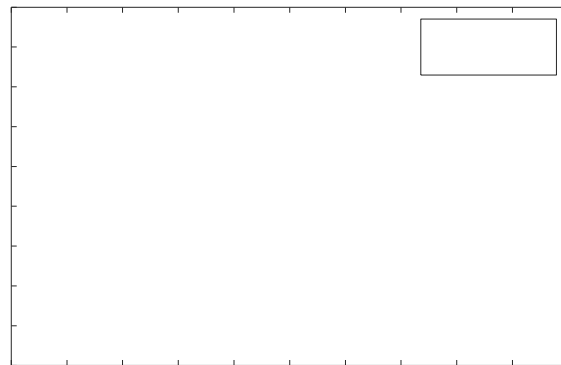


Figure 4: PSF profile of the first imaging lens.

Implementing the DMD

The DMD could not be directly implemented into the OTR imaging system as the large size of the micro-

mirrors restricted the number of resolution points across the PSF. To rectify this a two lens microscope system was introduced to provide an additional magnification factor prior to the DMD. Two additional lenses were placed between the DMD and the CCD for reimaging and calibration. It was important to ensure the quality of the PSF was maintained throughout the magnification optics. Any negative effect would be detriment to the resolution. The DMD and the associated reimaging optics were introduced after the initial optics [7]. A schematic of the HDR system is shown in Fig. 5.

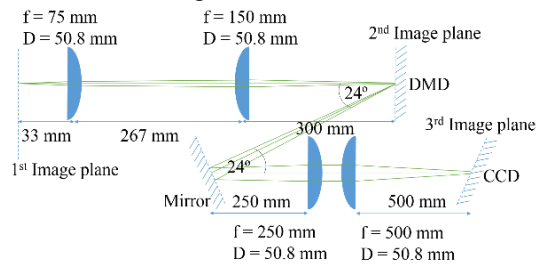


Figure 5: Schematic of the HDR imaging system.

The FWHM of the PSF was first measured at the 2nd image plane as $(2.6 \pm 0.2) \mu\text{m}$ with a magnification of 37. This resolution was comparable to the system in Fig. 3, which ensured that any change found in the PSF at the 3rd image plane was indeed caused by the DMD. To measure the PSF of the full optical system, a flat field digital mask was applied to the DMD, i.e. all mirrors at $+12^\circ$. A magnification of 17.8 and a resolution of $3.48 \mu\text{m}$ was measured using a resolution target.

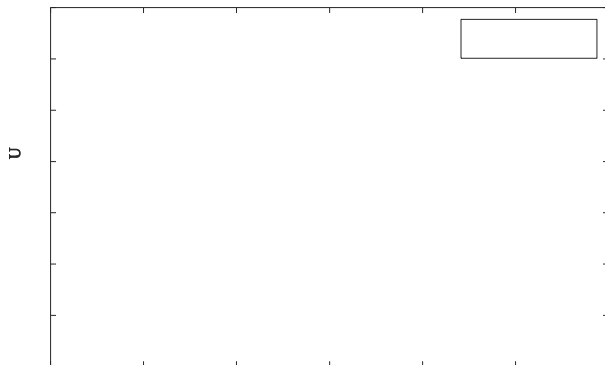


Figure 6: PSF profile of HDR system in flat field state.

The PSF profile and the fit Airy disk are presented in Fig. 6. There are no simulated results for this stage as simulating the effect the DMD has on the PSF is a non-trivial task [8] and remains to be determined. The measured resolution was $(2.4 \pm 0.2) \mu\text{m}$. The resolution of this system was comparable with the initial single lens imaging system, showing that the dominant factor in the PSF was the first lens in the optical system. This is a significant result. Neither the optics required for the DMD integration, nor the DMD itself, provide any measureable effect on the PSF. The resolution of the original system is maintained throughout the optics from the first lens to the CCD in Fig. 5.

CONCLUSION

The results achieved in this study are predicated on the creation and characterisation of a $(1.34 \pm 0.01) \mu\text{m}$ point source, using standard optics and a knife edge scan methodology. As the initial laser is a coherent light source, the point source itself is coherent. This is directly relevant for studying the coherent imaging of OTR, and to this end the point source was used to measure the PSF of an OTR imaging system. The FWHM of this distribution was $(2.99 \pm 0.01) \mu\text{m}$, which will significantly impair the attainable resolution when measuring micron size beams. However, this PSF can be used to remove this impairment via deconvolution. This presents the opportunity for sub-micron resolution measurements. To improve the PSF measurement of the optical system and the OTR profiles, a HDR imaging system was implemented after the original optics. This study has evidenced that the HDR optical components provide a negligible impact on the PSF of the original optical system. Further measurements are in progress to perform HDR measurements of both the PSF of the optical system using the point source, and the OTR profile. Future studies will also investigate the use of an incoherent point source, thereby allowing this entire process to be applied to any optical system.

REFERENCES

- [1] K. Kruchinin *et al.*, "Sub-micrometer transverse beam size diagnostics using optical transition radiation", *Jour. of Phys. Conf. Series*, vol. 517, no. 1, p. 012011, May 2014.
- [2] D. Xiang *et al.*, "Theoretical considerations on imaging of micron size electron beam with optical transition radiation", *Nucl. Instr. and Meth. in Phys. Res. A*, vol. 570, no. 3, p. 357-364, Jan. 2007.
- [3] S. Boogert *et al.*, "Micron-scale laser-wire scanner for the KEK Accelerator Test Facility extraction line", *Phys. Rev. ST Accel. Beams*, vol. 13, no. 12, p. 122801, Dec. 2010.
- [4] A. Siegman, "Defining, measuring, and optimizing laser beam quality", in *Proc. SPIE 1868, Laser Resonators and Coherent Optics: Modelling, Technology, and Applications*, Los Angeles, CA, USA, Jan. 1993, doi: 10.1117/12.150601.
- [5] A. Siegman, *Lasers*. USA: University Science Books, 1990.
- [6] M. Araújo *et al.*, "Measurement of Gaussian laser beam radius using the knife-edge technique: improvement on data analysis", *Applied Optics*, vol. 48, no. 2, p. 393-396, Jan. 2009.
- [7] H. Zhang *et al.*, "Beam halo imaging with a digital optical mask", *Phys. Rev. ST Accel. Beams*, vol. 15, no. 7, p. 072803, Jul. 2012.
- [8] X. Chen *et al.*, "Diffraction of digital micromirror device gratings and its effect on properties of tunable fiber lasers", *Applied Optics*, vol. 51, no. 30, pp. 7215-7220, Oct. 2012.